

Numerical modeling of stability of an embankment on clay subjected to rainfall – A case study in the city of Pucallpa

Modelación numérica de la estabilidad de un terraplén sobre arcilla sometido a precipitaciones – Un estudio de caso en la ciudad de Pucallpa

Oscar Alarcon

Carrera de Ingeniería Civil, Universidad de Lima, Perú, oscavar35@gmail.com

Marko López

Instituto de Investigación Científica, Carrera de Ingeniería Civil, Universidad de Lima, Perú

Roberto Quevedo

Tecgraf Institute at Pontifical Catholic University of Rio de Janeiro, PUC-Rio, Brazil

ABSTRACT: The city of Pucallpa, Peru, focuses its efforts on consolidating itself as one of the metropolises with the highest economic growth in Peru. Therefore, it must have an infrastructure that meets the technical requirements and standards of a modern city. Structures such as road embankment pavements have deteriorated rapidly during the rainy seasons because of problems caused by reduced soil resistance due to loss of suction. To understand these phenomena, several theories and formulations have been proposed that consider flow and deformation in unsaturated soils. However, only a few studies have explained them because of the complexity of the processes involved, resulting in conceptual deficiencies in the conception of infrastructure projects in Pucallpa. Thus, the lack of an adequate methodology for understanding and predicting the phenomena associated with unsaturated soils has become indispensable in geotechnical engineering. The main objective of this study is to analyze the stability of an embankment built on unsaturated clay soil under infiltration conditions caused by intense rainfall in the city of Pucallpa. The simulation results, carried out on finite element software Plaxis, show that the safety factor of the embankment is considerably reduced by punctual and long-lasting rainfall.

KEYWORDS: slope stability, rainfall infiltration, unsaturated soils, factor of safety, Plaxis

1 INTRODUCTION

Similar to any structure exposed to the environment, embankments can deteriorate; thus, their stability is affected as their service time is extended. A factor that compromises the stability of these structures is rainfall, as it can cause landslides due to the reduction in soil suction and an increase in interstitial pressure due to eventual elevations in the water table (Wang et al., 2020). Consequently, globally, several studies have been conducted to analyze the impact of rainfall on the stability of embankments. In the United States, in recent decades, there has been an interest in developing early warning mechanisms to prevent landslides (Godt et al., 2009) and avoid economic losses, including human lives. Although Peru has a completely variable geography that is different from that of other countries, this does not mean that similar problems do not arise. For example, in the tropical city of Pucallpa, temperature variations and intense rainfall generate floods and landslides that affect various communities.

The unsaturated condition of soil represents a challenge for the analysis of its deformation and resistance because of the limitations of conventional soil mechanics (Alfaro, 2008). The presence of solids, air, and water within the soil associated with very deep water tables generally increases the rigidity and strength of the soil. This initially stable situation can be compromised by rainwater infiltration, which significantly reduces the resistance of soil and increases its deformation

capacity. A compilation of geotechnical studies conducted in the city of Pucallpa has been presented by Lopez & Quevedo (2022), where most soils are categorized as clays of low and high plasticity. Their study also determined the deformability and resistance properties of these soils under saturated conditions. However, no studies have been conducted to determine the hydraulic and mechanical properties under unsaturated conditions. Therefore, the lack of knowledge of the interaction between structures built on unsaturated soil and natural phenomena has become a fundamental topic of study for the development of new construction projects.

To identify the behavior of different unsaturated soils, several studies have been conducted globally, some of which have investigated the direct influence of rainfall on the failure of slopes and embankments. Showkat et al. (2022) indicated that knowledge of the effects of infiltration and loss of suction on embankments is essential to determine their stability. Liu et al. (2017) performed different simulations of embankments of different heights to determine safety factors by analyzing the depth of damage caused by rainfall. Roshan et al. (2021) conducted tests to determine the properties and hydraulic characteristics of different soil samples that function as fill of an embankment to perform numerical modeling. Tu & Huang (2016) investigated the effect of rainfall infiltration on two embankments to determine the volumetric moisture content of soil and the variation in the interstitial pressure of these embankments and to obtain safety factors for each case. Quevedo et al. (2021)

analyzed the impact of climatic conditions on the stability of foundations built on collapsible soils.

The main objective of this study is to numerically analyze the effects of rainwater infiltration on the stability of an embankment built on a foundation of unsaturated soil in the city of Pucallpa. The Plaxis 2D software was used to simulate the behavior of the unsaturated soil in the model under study. There is also a parametric approach because the intensity and duration of rainfall vary according to data collected from government institutions in Peru. Finally, safety factors associated with embankment stability in various scenarios were determined.

2 SITE DESCRIPTIONS

The embankment under study is located in the city of Pucallpa, the capital of the department of Ucayali, in eastern to north-central Peru on the banks of the Ucayali River in the Amazon plain at 154 m above sea level. Since its foundation, multiple studies have been conducted in this territory to understand the behavior of its soils. In this sense, one of the tests that have generated the greatest impact in the determination of the strata that make up the territory of Pucallpa has been SPT drilling. Tests conducted by Alva (2013) indicate that, below the first layers of soil made up of clays, which in some areas reach up to 9 m deep, layers of silty sand have been detected. López & Quevedo (2022) conducted six recent explorations in which the minimum and maximum mechanical parameters of the clays were determined and moisture content ranging between 10% and 45% was obtained.

Some of the areas evaluated by these authors are shown in Figure 1, showing the drilling locations. Because of these tests, it was possible to determine the geological-geotechnical characteristics of the study area and the materials used for the simulations.



Figure 1: Satellite view of SPT test locations over Pucallpa.

Soils such as sand and clays are present in the study area; therefore, it is essential to know their behavior in an unsaturated state to evaluate different geotechnical analysis scenarios in the city. Although this study seeks to understand the landslides that may occur on an embankment influenced by the presence of rainfall, it is not a fact that only this type of analysis can be performed.

In the city of Pucallpa, a conventional meteorological station observes the surface and collects information, which is then transferred to the institutional database of the National Meteorology and Hydrology Service of Peru (Senamhi). This station is located in the Province of Coronel Portillo, belonging to

the district of Callaria, within the department of Ucayali. According to a report prepared for the Geological, Mining, and Metallurgical Institute, in 2008, the average annual maximum rainfall varied between 2000 and 8,000 mm (Núñez & Medina, 2008). As shown in Figure 2, the study area is located within a region of intense annual precipitation. Although the period is not considered for analysis, it allows us to obtain a value for comparison with future rainfall in the selected area.

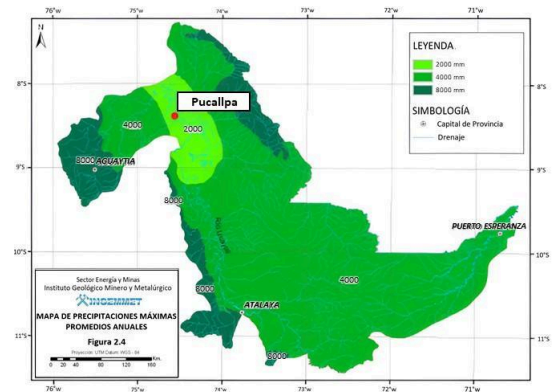


Figure 2: Map of maximum annual rainfall in 2008.

In this study, information about rainfall that occurred between 2018 and 2023 was collected. In addition, the intensity corresponding to the rainiest day during the study period of interest was selected, which corresponds to January 28, 2020, with a rainfall intensity of 189 mm/day. Simulations were performed to evaluate the effect of representative rainfall on the selected structure. Note that months with no data were considered null (0 mm) for improved calculations. In Figure 3, a record of rainfall is observed in January.

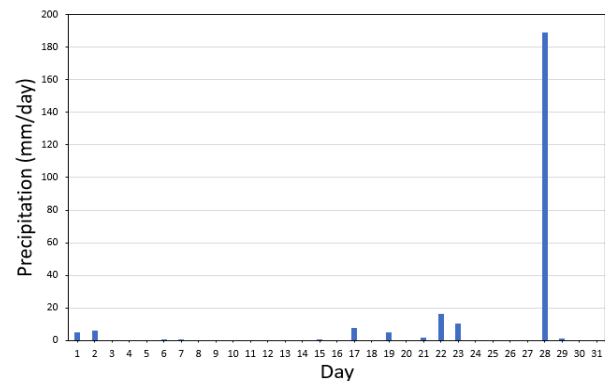


Figure 3: Rainfall intensity in January 2020.

3 UNSATURATED SOIL

3.1 Mechanical behavior

The principle of effective stress is the most important concept in soil mechanics (Wesly, 2018). Regarding unsaturated soils, the theory proposed by Terzaghi is not completely adequate, because it assumes that the soil is completely saturated. Thus, in search of

a better approach for the study of unsaturated soils, alternative stress variables have been used. For example, the net stresses and suction proposed by Fredlund & Morgestern (1977) or the generalized effective stresses initially proposed by Bishop (1959) and later elaborated by several authors. Both approaches provide a better approach to the analysis of practical problems in geotechnical engineering, such as slope stability, and include the effect of suction, which is important for understanding the behavior of unsaturated soils. In Plaxis, generalized effective efforts can be determined using Eq. (1).

$$\sigma' = \sigma - mu_a + m\chi(u_a - u_w), \quad (1)$$

where σ denotes the vector of total stresses, u_a and u_w denote the interstitial pressure of water and air, respectively, and m represents the vector that introduces the influence of pore pressure on effective stresses. χ denotes Bishop's parameter that defines the coupling between effective effort and suction. In Plaxis, this parameter is assumed to be the effective saturation (S_{eff}), which is described using Eq. (2),

$$S_{eff} = \frac{\theta_w - \theta_r}{\theta_s - \theta_r}, \quad (2)$$

where θ_w denotes the volumetric content of water, θ_s denotes the volumetric content of saturated water, and θ_r denotes the volumetric content of wastewater.

To represent stress-strain behavior, the Mohr-Coulomb model (MHC) was used, which is defined using the following plasticization function:

$$F_{MHC} = q - \left(p + \frac{c}{\tan \theta}\right)g_\theta, \quad (3)$$

where p represents the average effective effort, q represents the deflection effort, and g_θ denotes a function that depends on the Lode angle (θ). The three variables p , q , and θ denote the invariants of effective efforts. The parameters c and θ denote resistance properties, namely, cohesion and friction angle, respectively. For saturated conditions, the cohesion is similar to the effective one (c'). However, for unsaturated soils, the soil cohesion is assessed using Eq. (4).

$$c = c' + S_{eff}(u_a - u_w)\tan \theta \quad (4)$$

The friction angle is assumed to be independent of the soil suction as discussed in Fredlund et al. (2012). The plastic potential surface used for the determination of plastic deformations is similar to the surface defined using Eq. (3); however, the angle of friction is replaced by the angle of dilation (ψ). To complete the formulation of the model, a perfect plastic behavior defined by Young's modulus (E) and Poisson's coefficient (ν) is required.

3.2 Hydraulic behavior

To conduct flow analysis and understand the effect of soil suction on the final calculation of the safety factor, it is important to understand what this phenomenon consists of and the parameters involved. Suction is the ability of unsaturated soil to attract or retain water in terms of pressure and can be quantified in terms of

total suction (Ψ) (Fredlund & Rahardjo, 1993), as expressed using Eq. (5).

$$\Psi = (u_a - u_w) + \pi, \quad (5)$$

where the interstitial pressure of air (u_a) minus that of water (u_w) equals matrix suction, which is associated with capillarity caused by the surface tension of water; π denotes the osmotic suction associated with salts dissolved in the soil water. The latter can be omitted when solving geotechnical problems involving unsaturated soils. Therefore, for the proposed analysis, total suction is considered equal to matrix suction.

To estimate water flow and soil volumetric changes, the model proposed by van Genuchten (1980) was used to describe the soil water characteristic curve (SWCC), using Eq. (6).

$$\theta_w = \theta_r + \frac{(\theta_s - \theta_r)}{\left[1 + (a_{vg}\Psi)^{n_{vg}}\right]^{m_{vg}}}, \quad (6)$$

where a_{vg} , n_{vg} , and m_{vg} denote the tuning parameters for the van Genuchten model.

The SWCC represents the relationship between soil suction and some measures of water content (Zapata et al., 2000). Its determination for the two types of soils used in the simulation is possible owing to van Genuchten's model (van Genuchten, 1980).

Another fundamental equation for understanding the hydraulic behavior of unsaturated soils is the function of hydraulic conductivity or relative permeability (k_r), defined by Eq. (7).

$$k_r = \sqrt{S_{eff}} \left[1 - \left(S_{eff}^{1/m_{vg}}\right)^{m_{vg}}\right]^2. \quad (7)$$

This is described by Mualem's (1976) predictive model, which, along with van Genuchten's model, allows us to establish the parameter of the m_{vg} that determines the shape of the SWCC and the permeability function, as shown in Eq. (8).

$$m_{vg} = 1 - \frac{1}{n_{vg}}, \text{ when } 0 < m_{vg} < 1. \quad (8)$$

4 NUMERICAL MODELING

Numerical analysis with the Plaxis 2D software is performed using the finite element method assuming a flat state of deformation. The profile of the embankment is similar to that laid out in a study in Pucallpa, Peru. The soil of the foundation where the embankment is located is composed of clay and sand layers. Some simplifications were adopted in the model geometry in order to perform fast simulations. For example, the interface between clay and sand layers is assumed to be horizontal. In addition, because of the significant length of the structure outside the plane, a 2D model under plane strain conditions is adopted. Moreover, because of its structure, only half of the embankment is modeled, as shown in Figure 4. The shallowest clay layer, extends to a depth of 4.5 m, followed by a layer of sand that extends up to 11 m. Similarly, the water table is located 1.5 m below the sand. The model expands 15 m below the surface of the land to the right from the base of the embankment slope to avoid the effects of boundary conditions.

The mesh is composed of triangular elements of 6 nodes, each with 3 degrees of freedom associated with horizontal (u_x) and vertical (u_y) displacements and pore pressures (Gaber et al., 2018). The mesh size is refined locally on the embankment surface exposed to rain for improved numerical calculations. The

model has 1,154 elements. No sensitivity analysis was performed to determine the influence of contours or the size of these elements.

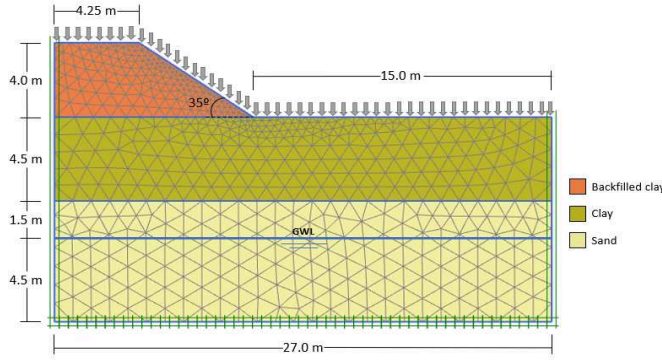


Figure 4: Slope geometry and boundary conditions.

In this case study, the mechanical boundary conditions of the fixed type or restricted displacements ($u_x = u_y = 0$) were established at the base of the model. Conversely, vertical movement was allowed on the sides parallel to the y-axis but not horizontally ($u_x = 0$).

Similarly, the hydraulic boundary conditions are defined throughout the model on the basis of the behavior of the movement of rainwater according to the different strata and the embankment. Thus, first, for extremes parallel to the y-axis and between the water table and the bottom of the first clay layer, the head condition is defined with initial and final values that allow changes in the water table even when the head remains constant over time. Conversely, the ends not considered as heads are assumed to be seepage that allows water to freely flow in and out of the ground.

Second, at the base of the model, there is a closed condition that defines a zero Darcy flux on the surface imposed by the application of Eq. (8).

$$q_x n_x + q_y n_y = 0, \quad (8)$$

where n_x and n_y denote the outward pointing normal vector components on the boundary.

Lopez & Quevedo (2022) collected data within the area delimited for this study, where the parameters to be used could be defined using the Mohr–Coulomb constitutive model. The parameters used are presented in Table 1 for each soil sample. In addition, an associated flow law was used, considering dilation angles similar to those of the friction angle.

Table 1: Soil parameters.

Material	Clay	Sand	Filler clay
Young's modulus—E (MPa)	30	15	50
Poisson's module— ν (-)	0.4	0.3	0.2
Effective cohesion— c' (kPa)	15	10	30
Friction angle— ϕ (°)	10.5	28	16
Unit weight— γ (kN/m ³)	18	16	18

Similarly, Table 2 presents the parameters necessary to generate the SWCC for each corresponding soil. The corresponding curves

for sand and clay are presented in Figures 5 and 6, respectively. Similarly, they are presented in Figures 7 and 8, where permeability is a function of matric suction.

Table 2: Hydraulic data for van Genuchten's model.

Soil	k_{sat} (m/day)	θ_r (-)	θ_s (-)	a_{vg} (1/m)	n_{vg} (-)	m_{vg} (-)
Sand	7.130	0.045	0.430	14.5	2.68	0.63
Clay	0.04750	0.068	0.380	0.8	1.09	0.08

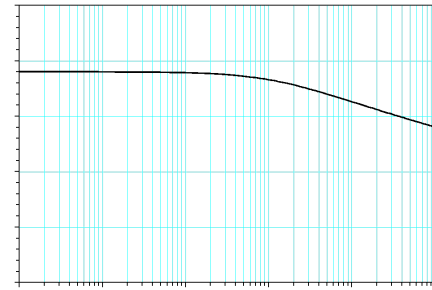


Figure 5: SWCC for clay soils.

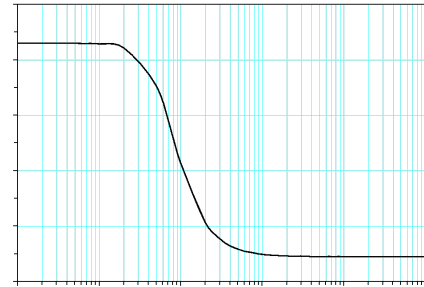


Figure 6: SWCC for sandy soils.

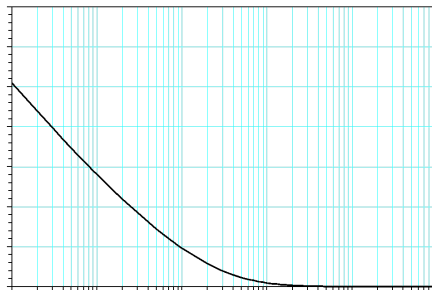


Figure 7: Permeability curve for clay soils.

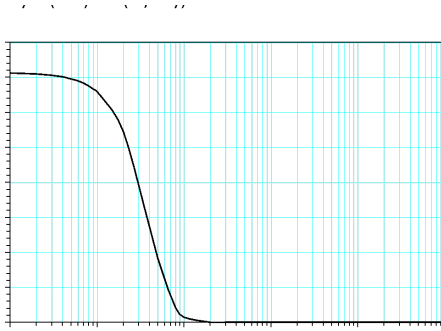


Figure 8: Permeability curve for sandy soils.

The model simulates the effect of rainfall on a 4-m-high embankment with a 35° slope through different phases. In the first phase, the already constructed embankment is presented and the initial effective forces, along with the interstitial water pressure, are calculated. These conditions are initialized on the basis of the weight of the embankment, a calculation process in Plaxis2D *Gravity Loading* to determine the initial stresses using the weight of soil. Figures 9 and 10 show the distribution of the vertical and horizontal effective forces, respectively, at the initial instant of the simulation.

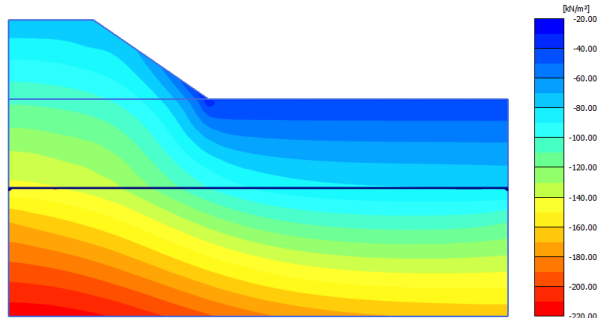


Figure 9: Distribution of initial vertical effective forces.

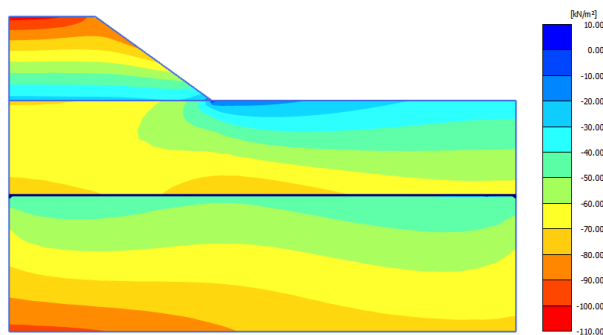


Figure 10: Distribution of initial horizontal effective forces.

Conversely, for pore pressure analysis, a type of calculation known as *steady-state groundwater flow* is used, which works with input parameters such as the water table, hydraulic boundary

conditions, and non-zero permeability for materials that constitute the model. Figure 11 shows the initial distribution of water pressures, with negative values below the water table and positive values above it.

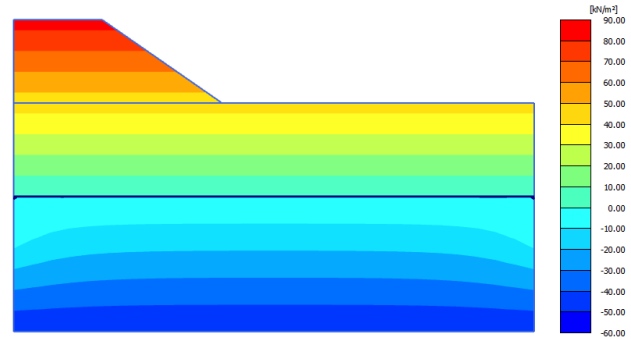


Figure 11: Initial distribution of water pressures.

Similarly, Figure 12 shows the corresponding initial suctions, which are null in regions completely saturated by water.

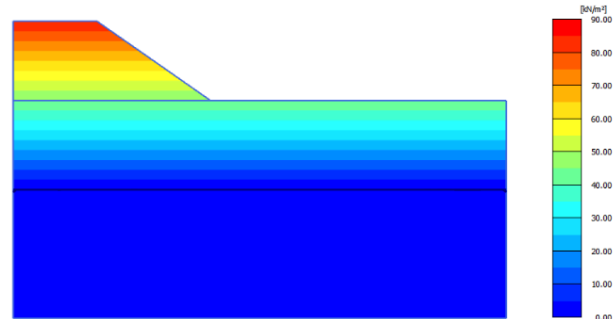


Figure 12: Initial distribution of suction.

Once the initial conditions for stresses and pore pressures have been established, during the second phase, rain infiltration over the top of the embankment is simulated using transient coupled analysis. A rainfall intensity of 189 mm/day was used during a total simulation period of 24 h. In this phase, the *fully coupled flow deformation analysis* function is used, which allows simultaneous simulation of soil deformation and variations in pore pressure, including the effect of suction on the calculation of effective stresses. This makes it possible to realistically assess the behavior of unsaturated soils through analysis that considers the reduction of permeability and its degree of saturation in unsaturated soil strata.

Finally, in the third phase, the safety factors for the embankment were determined using the shear strength reduction (phi/C reduction) method.

5 RESULTS AND DISCUSSION

To understand the impact of rainfall on the possible failure of the embankment, parametric analysis was performed in which the intensities and durations of the meteorological phenomena were varied. In addition, using the tools provided by Plaxis 2D, the

suction capacity of the soils that make up the embankment and the soil below it are jointly evaluated. Therefore, constant rainfall intensities with a value of 189 mm/day were simulated in intervals of durations of 4, 8, 12, 16, and 24 h.

Figure 13 shows the deformation of the model after 4 and 24 h of the onset of rainfall. An elastic swelling is observed, which is generated in the first 6 m adjacent to the base of the embankment. This phenomenon occurs when unsaturated soil absorbs water between its particles and expands in volume. Furthermore, it can be regarded as a part with an approximate height of 0.3 m for the first simulation and ending with a value of approximately 1 m for the elapsed 24 h.

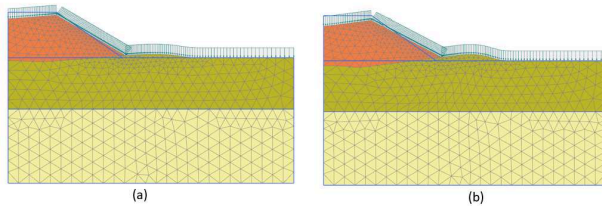


Figure 13: Deformed mesh for a) 4 h and b) 24 h.

The change in suction was also discussed. Because soils above the water table are considered unsaturated, they react differently to unexpected contact with rainfall. As rainfall prolongs, water infiltrates through the pores of the clay embankment and first layer, gradually increasing soil moisture. Similarly, because of the low permeability and inability of clay to absorb water, water mirrors are generated. This can be observed in Figure 14, where, compared with the initial suction presented, little infiltration is generated at the base of the embankment after 4 h of rainfall and sheets of water along the entire surface. Similarly, an increase in the water table is observed in a nonuniform way up to a height of 2.4 m compared with the initial level.

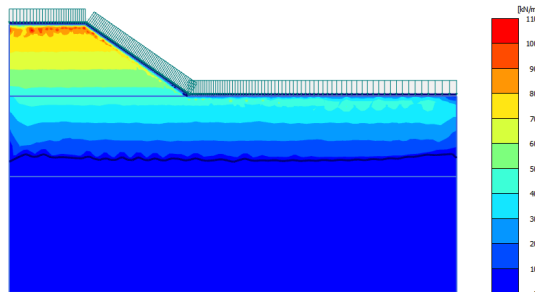


Figure 14: Suction for 4 h of simulation.

The information about the pore water pressure indicates variations along various points, as shown in Figure 15. This change in pressure occurs because the water table rises due to infiltration caused by rainfall. In noncompletely saturated soils, the pore pressure can be negative or positive, depending on the amount of air contained in the stratum under study. In this case, the maximum positive pressure reached 50 kPa in the initial state. However, as rainfall continues, this value increases, reaching approximately 105 kPa after 24 h of simulation.

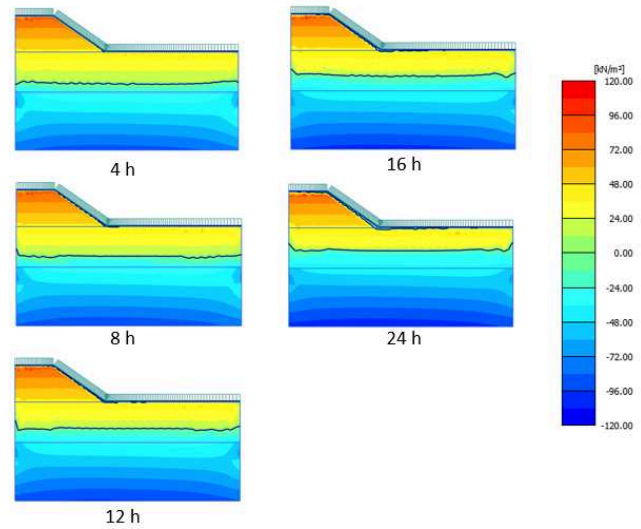


Figure 15: Pressure distribution of water pores over time.

Proceeding with more in-depth analysis of the pore water pressure, a series of Gaussian points at the top of the embankment were selected to assess the changes for the selected periods. Figure 16 shows the selection of points 208, 205, 334, and 383.

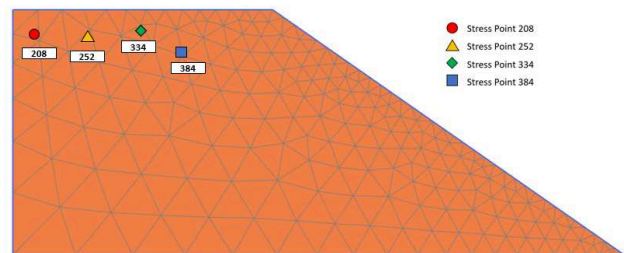


Figure 16: Gaussian points in the model.

Figure 17 shows the variation in water pore pressure (p_w) over time, i.e., as rainfall lasts longer. For points 208 and 334, there is a tendency for p_w values to increase, whereas for points 252 and 383, p_w values reach a peak and then decrease. This behavior can be seen in relation to the fact that the water table changes over time, i.e., it increases and decreases in some areas according to the duration of rainfall and the effects of soil suction. This fact alters the calculation of pore pressure and explains the different peaks that can be generated.

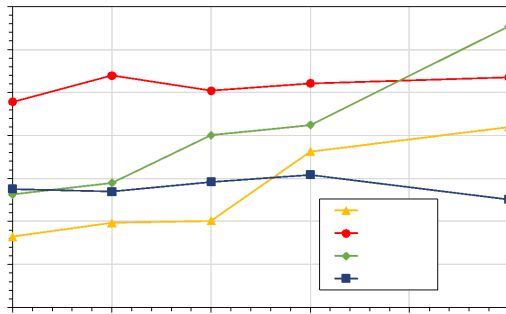


Figure 17: Variation in water pore pressure at different points on embankment.

The effect of rainfall on the embankment can compromise the stability of the structure. Therefore, the safety factors associated with the time of exposure to rainfall were evaluated in each calculation phase. Figure 18 shows the fault surfaces generated in the embankment for the initial and final simulation conditions, with an increase in the fault surface observed when the duration is 24 h.

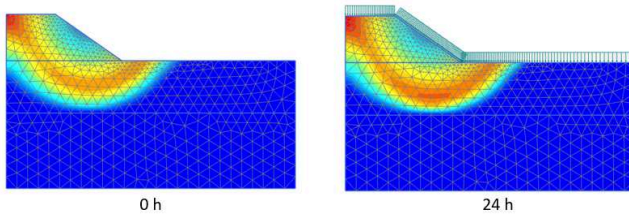


Figure 18: Fault surfaces for 0 and 24 h of precipitation.

Because it is coupled analysis, the calculation of the displacements caused by rainfall that directly affect the safety factor must be determined in the phase prior to the calculation of this factor. Figure 19 shows the maximum displacements for each rainfall duration.

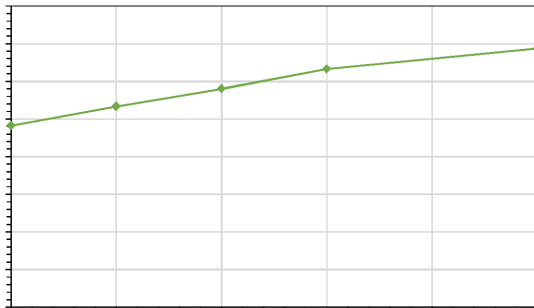


Figure 19: Maximum displacement as a function of time (h).

Figure 20 shows the evolution of the safety factor at different

points in the simulation. A progressive decrease in this factor can be observed as precipitation is prolonged over time. This is due to the loss of suction in unsaturated soils due to the infiltration of water into air voids, which reduces the apparent cohesion of soils and their stability. However, even at this precipitation intensity, the embankment remains stable ($FS = 2.4$) after 24 h of simulation.

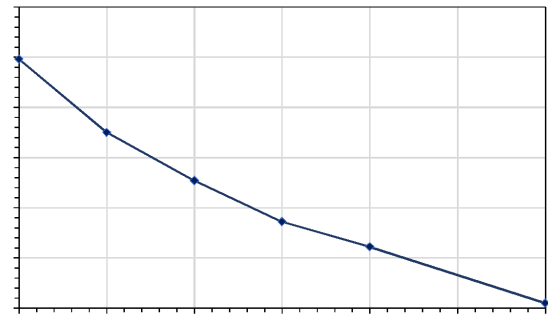


Figure 20: Safety factor as a function of time (h).

6 CONCLUSIONS

The effects of rainfall on embankments are phenomena that should be thoroughly investigated because they involve various factors that can complicate the analysis, ranging from the types of soils that make up the embankments to the climatic-environmental characteristics. Given that unsaturated soils require a different study approach than typical saturated soils, it is important to use appropriate techniques to develop more accurate numerical models that adequately represent the behavior of unsaturated soils.

The study of this phenomenon using numerical modeling allowed us to dynamically understand the behavior of embankments and their interaction with the environment. The transient coupled analysis was essential to develop an adequate interpretation of the deformation and changes in flow within the embankment, which may have been caused by rainfall in the study area. The selection of hydraulic boundary conditions according to the behavior of the soil below the structure was a fundamental step in the construction of a realistic model consistent with the effects of rainfall. Failure to understand this importance for future studies could lead to failure and misinterpretations of future scenarios.

Despite the simplifications adopted in the geometry of the model, our results show the impact of rainfall on the stability of the embankment under study through gradual reductions in the safety factor. These reductions can be explained by the loss of suction suffered by unsaturated soils during water infiltration processes. Similarly, the displacements and deformations that an artificial structure can experience compared with a natural structure are evident, because the premature design of embankments on unstable soil strata can prevent future failures. This is achieved through designs that consider the water table and its potential rise due to water infiltration effects. In contrast to

natural slopes, where the water table can occasionally be in close contact with the crest or the upper surface of the slope, enhancing their failure once they suffer load effects.

To avoid future disasters, it is recommended to continue studying unsaturated soils under climatic conditions. Extending the study area beyond Pucallpa, as well as the rainy season and the selection of intensities, can provide a better understanding of how unsaturated soils and embankments built on such soils behave. This would lead to the development of new methodologies for risk analysis and prevention.

ACKNOWLEDGEMENTS

The research presented in this paper was supported by *Instituto de Investigación Científica (IDIC) de la Universidad de Lima*. The authors wish to express their gratitude to the Geotechnics Laboratory of the *Universidad de Lima* for her great help in this work.

REFERENCES

- Alfaro Soto, M. A. (2023). GEOTECNIA EN SUELOS NO SATURADOS. Revista De La Academia Colombiana De Ciencias Exactas, Físicas Y Naturales, 32(125), 471–482. [https://doi.org/10.18257/raccefyn.32\(125\).2008.2315](https://doi.org/10.18257/raccefyn.32(125).2008.2315)
- Alva, J. (2013). “Estudios geotécnicos en la ciudad de Pucallpa”, Universidad Nacional del Ingenieria, 132. <http://www.jorgealvahurtado.com/files/EstudiosGeotecnicosPucallpa.pdf>. Accessed 26 February 2021
- Bishop, A. W. The principle of effective stress. Tek. Ukebl., vol. 106, no. 39, pp. 859–863, 1959
- Fredlund, D.G. and Morgenstern, N.R. (1977) Stress State Variables for Unsaturated Soils. Journal of the Geotechnical Engineering Division, 103, 447-446.
- Fredlund, D.G. and Rahardjo, H. (1993) Soil Mechanics for Unsaturated Soils. John Wiley and Sons, Inc., New York. <https://doi.org/10.1002/9780470172759>
- Fredlund, D., Rahardjo, H., Fredlund, M. 2012. Unsaturated Soil Mechanics in Engineering Practice. John Wiley & Sons, Inc.
- Gaber, M., Kasa, A., Abdul-Rahman, N., & Alsharif, J. (2018). Simulation of Sequential Construction of Embankments on Reinforced Soft Clay Foundation. Indian Geotechnical Journal. doi:10.1007/s40098-018-0317-3 Godt, J. W., R. L. Baum, and N. Lu (2009). Landsliding in partially saturated materials, Geophys. Res. Lett., 36, L02403, doi:10.1029/2008GL035996.
- Liu, J., Yang, C., Gan, J. et al. Stability Analysis of Road Embankment Slope Subjected to Rainfall Considering Runoff-Unsaturated Seepage and Unsaturated Fluid–Solid Coupling. Int J Civ Eng 15, 865–876 (2017). <https://doi.org/10.1007/s40999-017-0194-7>
- Lopez, M. & Quevedo, R. (2022). Modeling of Settlement and bearing Capacity of Shallow Foundations in Overconsolidated Clays. Journal of GeoEngineering, 17(1). [https://doi.org/10.6310/jog.202203.17\(1\).1](https://doi.org/10.6310/jog.202203.17(1).1)
- Muallem, Y. (1976). A new model for predicting the hydraulic conductivity of unsaturated porous media, Water Resour. Res., 12(3), 513–522, doi:10.1029/WR012i003p00513.
- Núñez Juárez, S.; Medina Allica, L. Geological risks in the Ucayali region. Lima: INGEMMET. 2008.
- Quevedo, R.; Romanel, C.; Roehl, D. Numerical modeling of unsaturated soil behavior considering different constitutive models. In MATEC Web of Conferences; EDP Sciences: Les Ulis, France, 2021
- Showkat, Rakshanda & Mohammadi, Hojjat & Babu, GL. (2022). Effect of Rainfall Infiltration on the Stability of Compacted Embankments. International Journal of Geomechanics. 22. 04022104. 10.1061/(ASCE)GM.1943-5622.0002425.
- Tu, G., & Huang, R. (2016). Infiltration in two types of embankments and the effects of rainfall time on the stability of slopes. Quarterly Journal of Engineering Geology and Hydrogeology, 49(4), 286–297. <https://doi.org/10.1144/qjegh2015-02>
- Van Genuchten, M.T. 1980. A closed-form equation for predicting the hydraulic conductivity of unsaturated soils. Soil Science Society of America Journal, 44: 892-898.
- Wang, Z., Li, Q., Zhang, N. et al. Slope failure of biotreated sand embankments under rainfall conditions: experimental investigation and numerical simulation. Bull Eng Geol Environ 79, 4683–4699 (2020). <https://doi.org/10.1007/s10064-020-01850-7>

- Wesley, L. (2018). Terzaghi, Bishop and the Practical Application of the Principle of Effective Stress. 2nd Chiam Teong Tee Memorial Lecture-cum-Lunch, IEM Academy, Wisma IEM, Petaling Jaya.
- Zapata, C., Houston, W., Houston, S. L. & Walsh, K., 2000. Soil-water characteristic curve variability.

INTERNATIONAL SOCIETY FOR SOIL MECHANICS AND GEOTECHNICAL ENGINEERING



This paper was downloaded from the Online Library of the International Society for Soil Mechanics and Geotechnical Engineering (ISSMGE). The library is available here:

<https://www.issmge.org/publications/online-library>

This is an open-access database that archives thousands of papers published under the Auspices of the ISSMGE and maintained by the Innovation and Development Committee of ISSMGE.

The paper was published in the proceedings of the 17th Pan-American Conference on Soil Mechanics and Geotechnical Engineering (XVII PCSMGE) and was edited by Gonzalo Montalva, Daniel Pollak, Claudio Roman and Luis Valenzuela. The conference was held from November 12th to November 16th 2024 in Chile.